Mem. S.A.It. Vol. 78, 108

Memorie della

Two-dimensional imaging of the He D_3/Hβ emission ratio in quiescent solar prominences

G. Stellmacher[1], E. Wiehr[2], and J. Hirzberger[3]

[1] Institute d'Astrophysique Paris, 98 bis Blvd. d'Arago, F-75014 Paris, France
[2] Institut für Astrophysik Friedrich-Hund-Platz 1, D-37077 Göttingen, Germany
e-mail: ewiehr@astro.physik.uni-goettingen.de
[3] Max-Planck-Institut für Sonnensystemforschung, D-37191 Katlenburg-Lindau, Germany

Abstract. Simultaneous prominences spectroscopy with THEMIS in the emission lines H-alpha, H-beta, HeD3, NaD2, Mgb2 and He(singlet)5015 lead to an extended study of two-dimensional images simultaneously in H-beta and HeD3. The spatial variation of the integrated line intensities and their ratio shows mainly two characteristics: (a) A constant emission ratio (even) in regions with substantial intensity variations; this can be explained by a varying number of superposing threads with equal physical states. (b) A varying emission ratio (often) tightly related to intensity changes; this indicates a superposition of threads with different physical states (most likely the gas-pressure). We also observe temporal changes of the emission ratio which seem to be too fast for a variation of the gas-pressure; here, we suppose a change of the packing density of threads along the line-of-sight which affects the penetration of ionizing UV radiation required for the He triplet excitation.

Key words. Sun: prominences – Sun: 2D-imaging – Sun: emission ratios

1. Introduction

The physical conditions in prominences may well be studied from images taken in the λ-integrated line intensities. The observation of such total intensities does not require the use of a spectrograph, but may be done with filters, just wide enough to also cover Doppler shifted line profiles. This enables a substantial decrease of the exposure time, thus higher spatial resolution and, hence, the investigation of fine-structures hardly visible in spectra. Model calculations of the emission ratios Ca II 8542/Hβ (Gouttebroze et al. 1997) and He D_3/Hβ (Labrosse & Gouttebroze 2001) showed the dependences on temperature, pressure and slab-widths. Wiehr and Stellmacher (1999) and Stellmacher and Wiehr (2000) observed simultaneous images in Ca II 8542 and Hβ and compared them with the model predictions. Here we present such observations in He D_3 and Hβ.

2. Observations

On July 14 and 15, 2003, we observed with the 1 m Swedish Solar Telescope (SST) on La Palma several quiescent prominences simultaneously in He D_3 and Hβ using a dichroic beam splitter and $\approx$2Å wide filters. The exposure time was set between 0.1 s and 0.25 s, accounting for the individual prominence bright-

Send offprint requests to: E. Wiehr

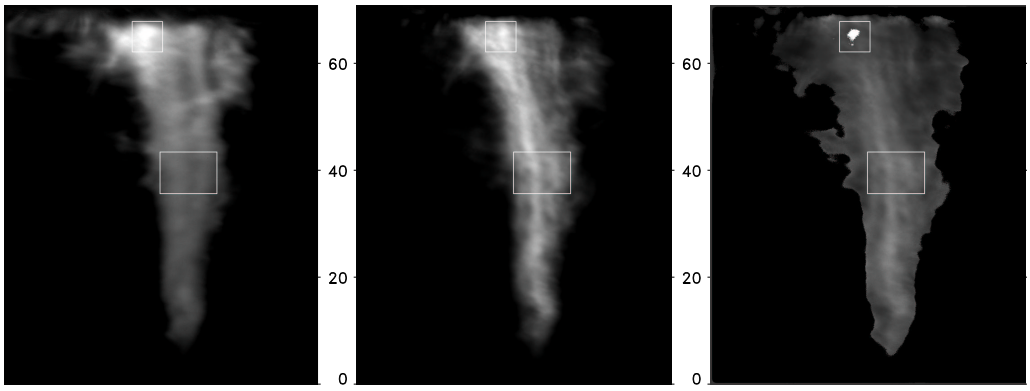

Fig. 1. Prominence at W/19N in the integrated light of the Hβ (left) and the He D_3 emissions (middle) together with their brightness ratio map (right panel); rectangles mark sub-fields with substantial evolution of the ratio; axes labels denote arc-seconds.

ness. Image motion was minimized using the correlation tracker of the SST, set to a nearby white light limb facular grain as lock-point. The raw images were corrected for the dark and the gain matrices; the underlying aureole was determined from the neighborhood of the respective prominence and subtracted. Two-dimensional maps of the emission ratio were obtained after spatial cross-correlation of the He D_3 and Hβ images.

3. Results

The finally obtained images and the corresponding ratio-maps allow a spatial and a temporal analysis. At the high spatial resolution achieved in the two-dimensional data (Figs. 1, 2), we mostly find small spatial variations of the He D_3/Hβ emission ratio over the whole prominences. Fig. 1 shows a prominence at W/19N which has been observed through 12.3 min thus allowing to compare the temporal evolution of the emission ratio with that of the integrated line intensities.

For a more detailed discussion, we give scatterplots of the emission ratio versus the He D_3 and, respectively, the Hβ total intensities for selected sub-fields of the observed prominences. These scatterplots (Figs. 3 through 5) show a clustering of data points indicating the spatial prominence structure in the respective sub-field.

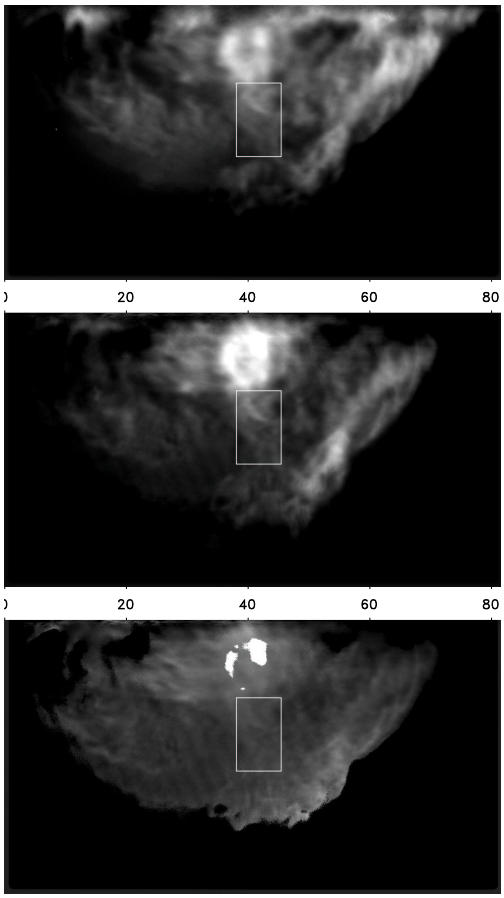

Fig. 2. Same as Fig. 1 but for a prominence at E/55N.

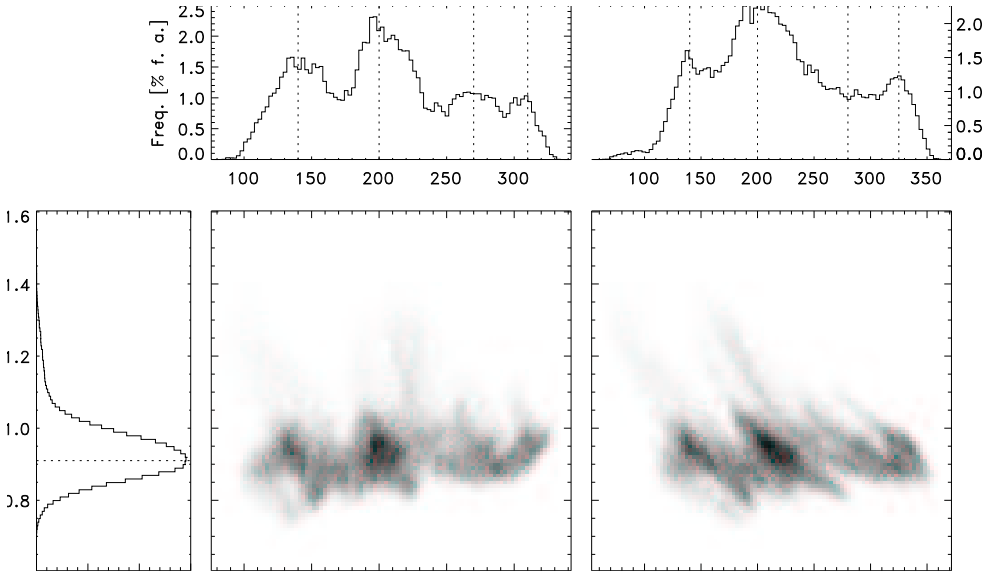

Fig. 3. Scatterplot of the He D_3/Hβ ratio versus the total intensities of He D_3 (middle) and Hβ (right panels) for the sub-field in prominence E/55N from July 14, 2003, (cf., Fig. 2); cumulations of data points are indicated by vertical lines in the corresponding number histograms (at the top, obtained from integration along the ordinate); they indicate different numbers of threads along the line-of-sight. The ratio histogram (at the left side, obtained from integration along the abscissa) shows a single-peaked distribution in spite of the marked intensity structure .

This clustering is well seen in histograms obtained by integrating the scatterplots along their ordinates (panels on top of the scatterplots). Distinct maxima of the intensity histograms, marked by vertical lines, frequently occur in prominences (Stellmacher & Wiehr, 2000) and are attributed to a spatially varying number of threads along the line-of-sight (LOS).

3.1. Spatial ratio behavior

Interestingly, such pronounced spatial brightness structure does not necessarily occur in the ratio of the emission lines which, instead, is often found to be almost constant, even in sub-regions with marked intensity variation. In such cases, the prominence structure appears rather similar in both lines, resulting in a largely uniform emission ratio independent from the structure (Fig. 3). We also find prominence regions where the structure is much more pronounced in the one than in the other line. Figure 4 gives an example for an inverse dependence of the ratio on the Hβ brightness, since the He D_3 distribution is single-peaked. In contrast, the prominence given in Fig. 1 shows an almost unique Hβ brightness, the ratio map thus being largely similar to the He D_3 structure.

In summary, the spatial variations of the He D_3/Hβ emission ratio may (A) be *constant* for the (trivial) case (A1) that both emissions are constant and (A2) that they exhibit very similar spatial variations; it may (B) *vary* parallel with the He D_3 intensity (B1) or inversely with the Hβ intensity (B2). With regard to the clustering of data points in the scatterplots, both scenarios may be explained by different numbers of threads along the line-of-sight with (A) largely equal or (B) different intrinsic atmospheric states.

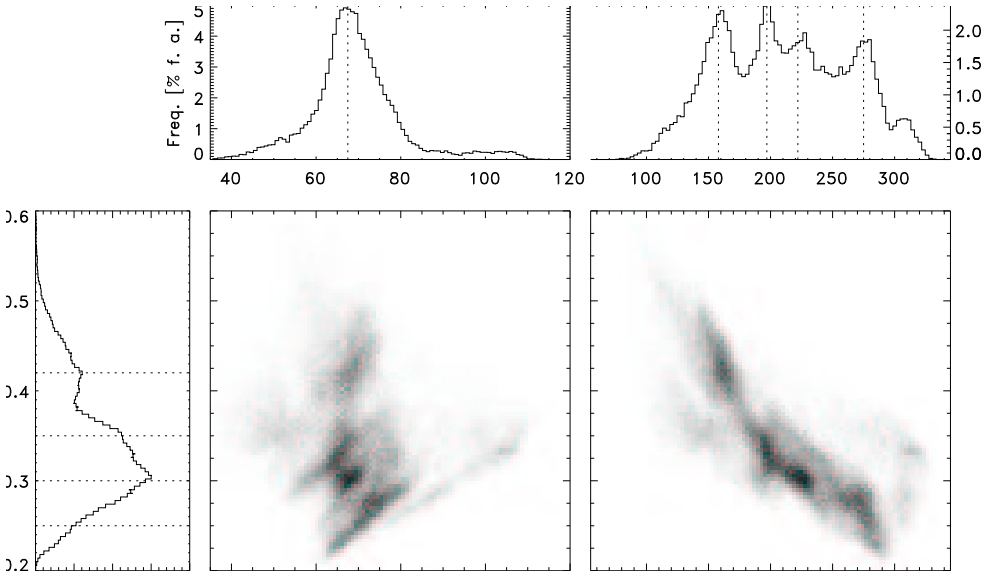

Fig. 4. Same as Fig. 3 but for a sub-field in a prominence at E/31S from July 14, 2003, (note shown here); the intensity histograms indicate a marked structuring of the Hβ emission, but a single-peaked distribution for He D_3 (upper panels); the ratio histogram thus largely reflects the inverse Hβ structuring .

3.2. Temporal ratio behavior

In order to further check such an explanation, we also study the temporal behavior of the He D_3/Hβ emission ratio as deduced from the (short) time series of some prominences observed. The one at W/19N is observed through 12.3 min; in a sub-field, marked by the upper rectangle in Figure 1, the *He D_3 maximum intensity increases* (from 310 to 380 counts; cf., Figures 4 and 5), whereas the *Hβ minimum intensity decreases* (from 410 to 340 counts); accordingly, the upper limit of the emission ratio increases from 0.67 to 0.80 (cf., Figures 4 and 5). We similarly find other prominence sub-fields where the (relative) line intensities exhibit substantial evolution while the emission ratios either vary with time or remain unchanged.

4. Discussion

If we apply the idea of different thread numbers along the line-of-sight (LOS) as source of the 'structured' intensity histograms to the observed *temporal variation* of the histogram maxima, it indicates a 're-arrangement' of threads along the LOS as, e.g., described by Engvold (1997). For prominence regions where intensity variations are *not* accompanied by substantial changes of the emission ratio, the various superposing threads will be of nearly equal physical state. Since both emission lines are optically thin, a superposition of a (spatially or temporally) varying number of threads along the LOS will change the total line intensity. The emission ratio will remain unchanged if the threads exhibit equal intrinsic physical states.

If, however, the emission ratio is observed to be related to a (spatial or temporal) intensity modulation, the superposing threads will have different intrinsic physical states. The physical parameters responsible for various observed He D_3/Hβ emission ratios have been discussed by Labrosse and Gouttebroze (2001). Their calculations show, from 1-D slab models, that the ratio mostly depends on the gas pressure, less on slab width and temperature. At locations with rather fast temporal changes and, in particular, such with *opposite*

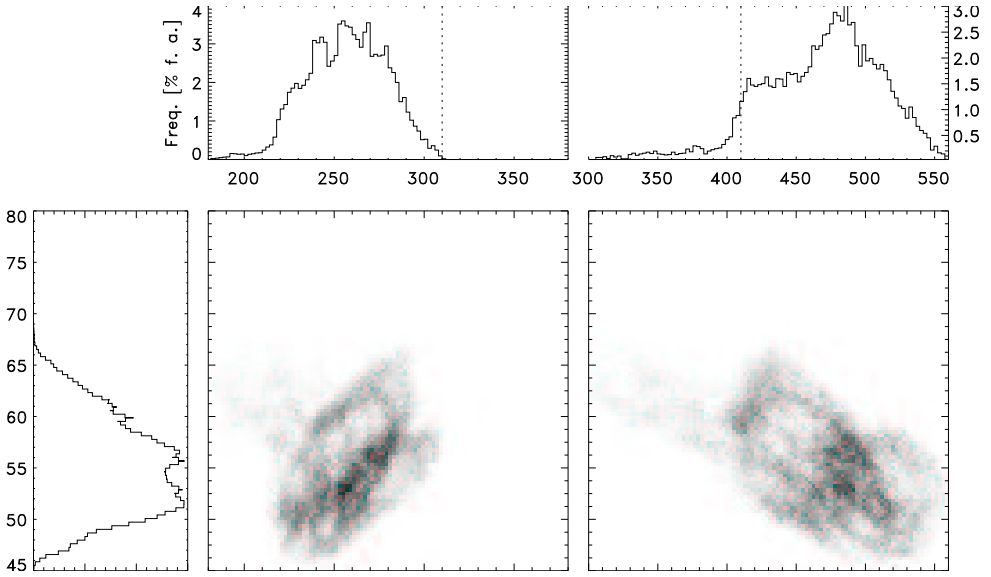

Fig. 5. Same as Fig. 4, but for the upper sub-field of prominence W/19N (Fig. 1).

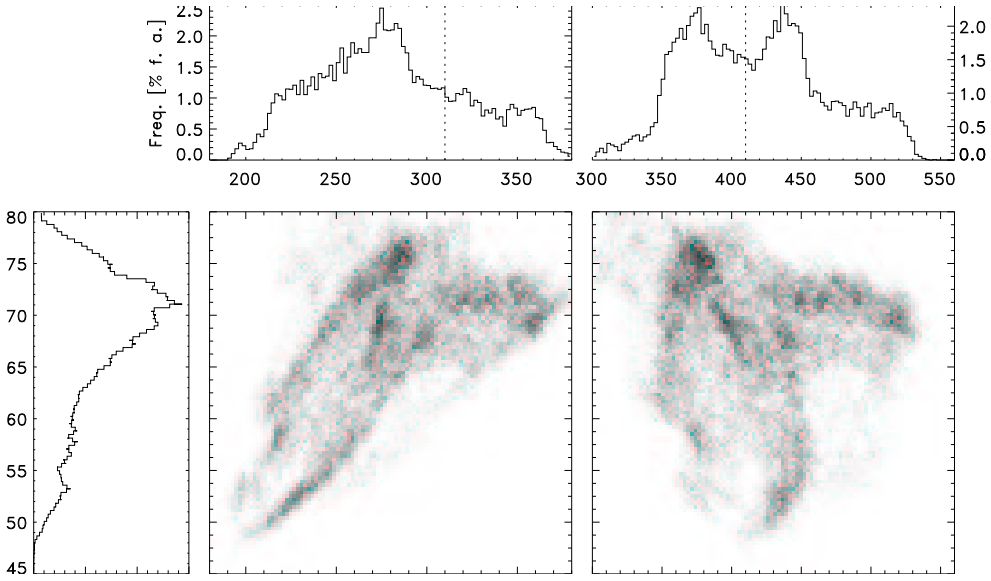

Fig. 6. Same as Fig. 5, but 12.3 min later.

brightness evolution as in Figure 5, we rather assume a change of the spatial density of the sub-structures within each thread. Larger distances between them (i.e., a smaller packing density) allow a deeper penetration of ionizing EUV radiation which affects the population of the He I triplet system and thus the rate of the He D_3 excitation. Another possible explanation might be a different saturation of the two lines: if several threads superpose along the

LOS yielding larger total τ values, the emission ratio will vary depending on the number of threads - even for similar intrinsic conditions. This has to be verified by modeling of the two lines.

5. Conclusions

Our two-dimensional observations confirm, at the high spatial resolution achieved with SST, the spectroscopic ('one-dimensional') results by Stellmacher and Wiehr (1994, 1995, 2005) and by de Boer, Stellmacher and Wiehr (1998), that prominences show emission ratios of the Helium triplet to the Hydrogen Balmer lines with a relatively low scatter around a characteristic (local) mean. Indeed, we find extended locations within prominences with a rather constant ratio (i.e. homogeneous gray in the ratio maps); the widths of those ratio distributions (cf., histograms) are compatible with the scatter in the spectral results. However, we also find prominence regions with substancial variations of the emission ratio both in space and time.

The analysis of prominence images obtained simultaneously in the integrated He D_3 and the Hβ lines well shows that the intensity variation over solar prominences, cannot be explained by a simple stationary radiative state alone. It reflects a complex relation between its fine-structure and the magnetic field (including MHD waves and oscillations; see also Engvold, 2004).

The role of the magnetic field as possible source of such spatial and temporal behavior of the He D_3/Hβ emission ratio can best be studied from well resolved magnetic field measurements. Since slit spectroscopy of the Zeeman effect (e.g. Kim et al. 1984) requires rather long exposures, two-dimensional observations of the Hanle effect (cf., Wiehr and Bianda 2003) may be more suitable.

Acknowledgements. We thank the SST staff for valuable help with the instrument. The 1 m Swedish Solar Telescope is operated by the Swedish Academy of Science at the Spanish Observatorio del Roque de los Muchachos (IAC). This project has been supported by the European Commission through the Instituto de Astrofsica de Canarias to fund the European Northern Observatory, in the Canary Islands.

References

De Boer, C. R., Stellmacher, G., & Wiehr, E. 1998, A&A 334, 280

Engvold, O. 1997, in Proceedings of 'New Perspectives on Solar Prominences', Aussois, eds. D. Webb, D. M. Rust, B. Schmieder, p.23

Engvold, O. 2004, Proceedings IAU Symp. No. 223, 187

Gouttebroze, P., Vial, J. C., & Heinzel, P. 1997, Solar Phys. 172, 125

Kim, I. S., Koutchmy S., Stellmacher G., & Nikolsky, G. M. 1984, A&A 140, 112

Labrosse, N.,& Gouttebroze, P. 2001, A&A 380, 323

Stellmacher, G. & Wiehr, E. 1994, A&A 286, 302

Stellmacher, G. & Wiehr, E. 1994, A&A 299, 921

Stellmacher, G. & Wiehr, E. 2000, Solar Phys. 196, 375

Wiehr, E. & Stellmacher, G. 1999, ESA conf. SP-448, p. 435, (ed. A. Wilson)

Wiehr, E., Bianda, M. 2003, A&A 404, L-25